Multistep Compositional Remodeling of Supported Lipid Membranes by Interfacially Active Phosphatidylinositol Kinases

Seyed R. Tabaei,[†] Feng Guo,[‡] Florentine U. Rutaganira,[§] Setareh Vafaei,[†] Ingrid Choong,[‡] Kevan M. Shokat,[§] Jeffrey S. Glenn,*[,‡,||] and Nam-Joon Cho*[,†]

[†]School of Materials Science and Engineering and Centre for Biomimetic Sensor Science, Nanyang Technological University, 50 Nanyang Avenue, 639798, Singapore

[‡]Departments of Medicine, Division of Gastroenterology and Hepatology, and Microbiology & Immunology, Stanford University School of Medicine, Stanford, California 94305, United States

[§]Howard Hughes Medical Institute, Department of Cellular and Molecular Pharmacology, University of California San Francisco, San Francisco, California 94158-2280, United States

[||]Palo Alto Veterans Administration Medical Center, Palo Alto, California 94304, United States

S *Supporting Information*

ABSTRACT: The multienzyme catalytic phosphorylation of phosphatidylinositol (PI) in a supported lipid membrane platform is demonstrated for the first time. One-step treatment with PI 4-kinase IIIβ (PI4Kβ) yielded PI 4-phosphate (PI4P), while a multistep enzymatic cascade of PI4Kβ followed by PIP 5-kinase produced PI-4,5-bisphosphate (PI(4,5)P$_2$ or PIP2). By employing quartz crystal microbalance with dissipation monitoring, we were able to track membrane association of kinase enzymes for the first time as well as detect PI4P and PI(4,5)P$_2$ generation based on subsequent antibody binding to the supported lipid bilayers. Pharmacologic inhibition of PI4Kβ by a small molecule inhibitor was also quantitatively assessed, yielding an EC$_{50}$ value that agrees well with conventional biochemical readout. Taken together, the development of a PI-containing supported membrane platform coupled with surface-sensitive measurement techniques for kinase studies opens the door to exploring the rich biochemistry and pharmacological targeting of membrane-associated phosphoinositides.
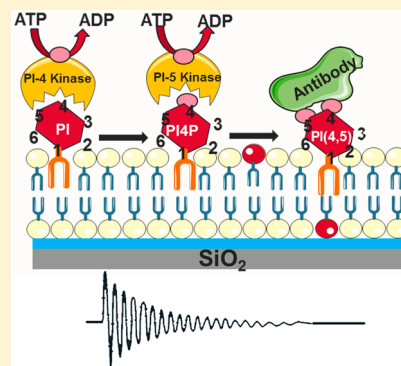
Phosphatidylinositol 4-kinases (PI4Ks) are a family of enzymes catalyzing the phosphorylation of phosphatidylinositol (PI) at the D-4 position of the inositol headgroup, producing phosphatidylinositol 4-phosphate (PI4P), which serves as a precursor for other important phosphoinositides (PIs) such as phosphatidylinositol 4,5-bisphosphate [PI(4,5)-P$_2$] and phosphatidylinositol (3,4,5)-trisphosphate [PI(3,4,5)-P$_3$], which are central to signal transduction and membrane trafficking.[1] Among this class of enzymes, PI4K mainly localizes at the Golgi and is vital for organelle formation and function.[2] Increasing evidence of involvement of PI4Ks in the pathogenesis of several diseases has prompted significant interest to identify potent and selective inhibitors for individual PI4Ks.

To study lipid kinases, conventional assays utilize PI in a nonbilayer format in either a micellar form in the presence of a detergent[3] (e.g., Triton-X) or lipid blot on a hydrophobic surface (e.g., nitrocellulose). However, the lipid kinase is naturally active at the water−lipid interface of cellular membranes and the physical properties of the membrane such as fluidity and membrane compositional features (e.g., domains) are likely to influence the activity of the enzyme. Lipid vesicles containing PI have also been used as lipid kinase substrates.[4] However, experiments using vesicles in suspension might be convoluted and disturbed by vesicle aggregation and/or fusion.[5]

Supported lipid bilayers (SLBs)[6] represent a simplified, two-dimensional model membrane that mimics key properties of biological membranes. So far, SLBs have not been utilized to study membrane association of PI kinases despite the analytical merits of employing surface-sensitive measurement approaches and the recent progress achieved in preparing SLBs which contain low PI fractions.[7,8] The only related study to date was reported by Debjit et al.[9] and involved using radiolabeled ATP in order to measure the final conversion yield of PI(4,5)P$_2$ to PI(3,4,5)P$_3$ for a kinase-treated SLB.

Here, we demonstrate for the first time the multistep enzymatic activity of PI lipid kinases on PI-containing SLBs using quartz crystal microbalance with dissipation monitoring (QCM-D)[10] measurement technique. The QCM-D enables real-time monitoring of adsorption processes involving proteins and lipid membrane interfaces.[11−13] We are able to detect membrane association of kinase enzymes and track enzymatic

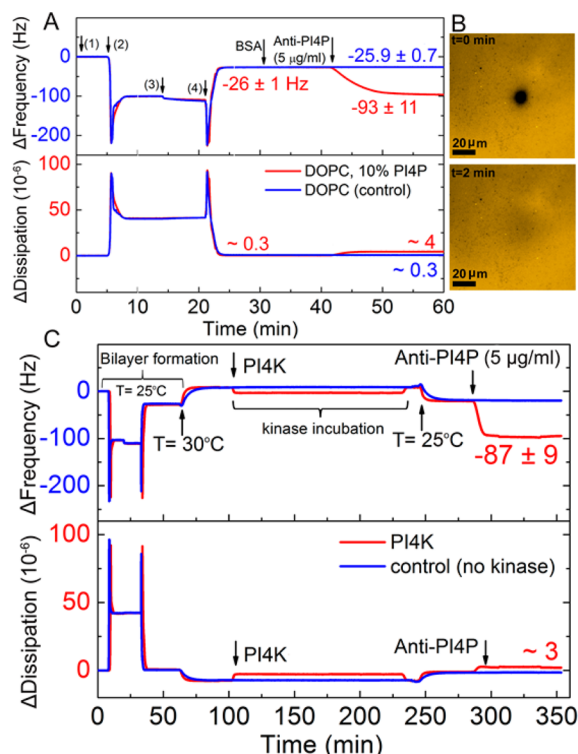conversion of PI substrates based on single- and multistep enzymatic processes.

The SLBs are prepared by the solvent-assisted lipid bilayer (SALB)[14] formation process, which is a vesicle-free method.[15] A representative experimental trace for formation of a DOPC bilayer doped with PI4P is presented in Figure 1A. Once the

Figure 1. (A) QCM-D frequency shift (ΔF, top panel) and dissipation (ΔD, bottom panel) for the third overtone were measured during formation of pure DOPC bilayer (blue curve) and DOPC bilayer doped with PI4P (red curve) on SiO$_2$ using the SALB method. Arrows indicate the injection of (1) buffer (10 mM Tris, 150 mM NaCl, pH 7.5), (2) isopropanol, (3) lipid mixture [0.5 mg/mL of DOPC in isopropanol with or without 10% PI4P (dissolved in ethanol)], and (4) buffer solution. Subsequently BSA protein (0.1 mg/mL) was injected. (B) FRAP snapshots of PI4P doped bilayer containing 0.5 wt % Rho-PE lipid. (C) PI containing bilayer was formed at room temperature (25 °C) and incubated with PI4K in kinase buffer [20 mM Tris (pH 7.5), 5 mM MgCl$_2$, 2 mM DTT, 0.5 mM EGTA, 100 μM ATP] (red trace) or buffer alone (blue trace) at 30 °C. Finally anti-PI4P was injected to verify enzymatic conversion of PI to PI4P. The average frequency shift of four experiments is given. Schematic illustration of the process is depicted in Figure S3.

SALB procedure was finished (t = 25 min), the ΔF and ΔD values were consistent with an SLB.[16] The BSA adsorption onto the bilayers resulted in a ΔF of <−2 Hz, indicating low defect density. To verify successful incorporation of PI4P, anti-PI4P antibody was injected in order to monitor antibody-based detection. Injection of anti-PI4P IgM resulted in a dramatic decrease in the resonance frequency (ΔF = 67 ± 12.6 Hz), suggesting an increase in the mass of membrane due to the adsorption of the antibodies. By contrast, injection of the same antibody to a 100 mol % DOPC bilayer resulted in almost no frequency shift, indicating no mass increase on the DOPC lipid bilayer and confirming specific detection of PI4P. FRAP on this bilayer (Figure 1B), further verified the formation of a fluid lipid bilayer with a lipid diffusivity of 1.8 μm^2/s (see the

Supporting Information for experimental details). The same procedure was successfully applied to form a DOPC lipid bilayer doped with PI and PI(4,5)P$_2$ (see Figures S1 and S2).

Next we determined the ability of PI kinases to generate their enzymatic product *in situ* by treating PI-containing bilayers with PI kinase enzyme (Figure 1C). Briefly, after formation of bilayers containing PI substrate as above, the temperature was raised to 30 °C. The kinase reaction was conducted at 30 °C because, based on previous reports,[17] the maximum kinase activity occurs at this temperature. For the QCM-D measurements that are operated in a liquid environment, the frequency and dissipation responses are affected by the bulk properties (viscosity and density) of the liquid.[18] Therefore, increasing temperature from 25 to 30 °C resulted in a positive and a negative change in the resonance frequency and energy dissipation, respectively, due to a change in the bulk viscosity. Next, the buffer was exchanged to kinase buffer followed by injection of PI4K. Next the buffer was exchanged to the original buffer and the temperature was set to 25 °C. To detect PI4P generation, anti-PI4P was injected.

Upon incubation with kinase (2.5 nM), a frequency shift of ∼12 Hz was observed (Figure 1C). The proportion of the enzyme which is bound to the interface is an important determinant of the kinetic of interfacially active enzymes. The enzyme in the aqueous solution first binds to the membrane and forms a complex with the lipid substrate, engaging in catalytic activity. After this step, depending on the membrane environment, e.g., surface charge density, the enzyme either detaches from the interface and goes back to the aqueous phase or binds another substrate molecule at the same interface.[19] There is evidence that some lipid kinases tightly bind to highly charged anionic vesicles that are purely composed of phosphoinositols or other negatively charged lipids.[20] This observation further shows that surface-sensitive analytical tools such as QCM-D can be effectively applied to supported lipid bilayers to investigate the interaction of interfacially active enzymes with membranes in a label-free measurement format.

Antibody binding to bilayers treated with PI4K led to a decrease in ΔF until it reached a final value of −87 ± 9 Hz. A control experiment was also performed in which no enzyme was included in the kinase buffer. In that case, no antibody binding was observed, indicating that the aforementioned antibody binding was specific for newly generated PI4P. We also performed another control experiment by adding anti-PI(3,4,5)P$_3$ antibody (as a specificity control) to bilayers containing 10% PI lipids that were exposed to PI4K kinase. In contrast to the case when anti-PIP antibody was added (Figure 1C), almost no binding was observed upon anti-PI(3,4,5)P$_3$ addition (Figure S4), indicating the specificity of the assay. In addition, washing with buffer after antibody binding, resulted in <2 Hz positive shift in the frequency in the course of ∼20 min (Figure S5), indicating a minute nonspecific binding.

To calculate a conversion yield for the percentage of phosphatidylinositol lipids converted to PI4P on a supported bilayer that contains 10% PI lipids, we compared the amount of anti-PI4P IgM bound to bilayers containing 10% PI4P with that of bilayers containing 10% PI lipids after exposure to the kinase. Since antibodies are not perfectly rigid, the relationship between frequency shift and adsorbed mass may not obey the Sauerbrey equation. Thus, we used the QCM-D experimental data collected at the third, fifth, seventh, and ninth overtones and analyzed them by using the Voigt-Voinova model,[21] as previously reported.[22] A summary of viscoelastic modeling

result for antibody binding to PI4P-containing membranes is presented in Table S1. By assuming an anti-PI4P IgM molecular weight of 970 kDa, the number of antibodies bound to bilayers containing 10% PI4P and bilayers containing 10% PI lipids after exposure to the kinase are $14\,621 \pm 477/\mu m^2$ and $12\,885 \pm 754/\mu m^2$, respectively. Thus, a conversion yield of 88% (the ratio of the two numbers) was calculated. Since the PI lipids facing the sensor surface are inaccessible to the enzyme, the enzyme-catalyzed PI conversion reactions are most likely occurring in the upper leaflet only and thus the calculated reaction yield corresponds to the percentage of PI lipids on the top leaflet of the bilayer that have been phosphorylated.

To further extend the complexity of enzymatic conversion of PI in the bilayer platform, we investigated the generation of $PI(4,5)P_2$ by sequential treatment of a PI-containing bilayer with a PI4 kinase followed by a PIP5 kinase. The SLB containing PI was prepared by the SALB method and used as a substrate for PI4Kβ, as described above (Figure 2B). Next, in situ generated PI4P was converted to $PI(4,5)P_2$ by injection of PIP5K1α. The generation of $PI(4,5)P_2$ was monitored by specific anti-$PI(4,5)P_2$ binding to the treated bilayer. As a control experiment, the same protocol was repeated except the incubation step with PIP5K1α (Figure 2B, dashed line). Injection of anti-$PI(4,5)P_2$ IgM to the PI-containing membrane treated only with PI4Kβ, resulted in a frequency shift of about -5 Hz. Antibody binding to the bilayer which was treated with both PI4K and PIP5K resulted in a frequency shift of about ~ -33 Hz. Importantly, the binding in this case did not reach a saturation level in our experimental time scale. These observations indicate that even though a small fraction of anti-$PI(4,5)P_2$ binds to PI4P, the majority of the antibody binding signal originates from binding to $PI(4,5)P_2$. Using viscoelastic modeling, the number of membrane-bound anti-$PI(4,5)P_2$ IgM was calculated to be $8558/\mu m^2$. By comparing this value with the number of antibodies expected to bind to the bilayers containing 10% PI lipids treated with PI4K kinase ($12885/\mu m^2$) (Table S1), a yield of 66% for conversion of PI4P to $PI(4,5)P_2$ was calculated.

Additional confirmation of the generation of $PI(4,5)P_2$ was obtained by fluorescence detection of in situ generated $PI(4,5)P_2$. Figure 2C−E presents background-corrected fluorescence microscopy images for a DOPC lipid bilayer doped with PI and $PI(4,5)P_2$ and a bilayer containing PI which was treated sequentially with PI4Kβ and PIP5Kα, respectively, incubated with fluorescently labeled anti-$PI(4,5)P_2$ antibody. As expected, the anti-$PI(4,5)P_2$ antibody did not bind to the PI-containing bilayer, with negligible signal (Figure 2C).

On other hand, there is significant antibody staining apparent on the treated SLBs, as denoted by a relatively bright fluorescence signal. In addition, there are a few unevenly distributed antibody clusters which appear as particularly brighter spots. The observed aggregates might be due to the formation of phosphoinositide clusters, which have been previously reported for PIP-containing model membranes in the presence of divalent cation[23] such as Mg^{2+} that is present in the kinase buffer. The formation of $PI(4,5)P_2$ clusters also might affect the binding kinetics for anti-$PI(4,5)P_2$. Compared to the binding kinetics of anti-PI4P (Figure 1C), the binding kinetics of anti-$PI(4,5)P_2$ is slower and quasi-linear (Figure 2A). Considering the large size of IgM, (a mushroom-shaped molecule of around 35 nm),[24] the initial binding to a cluster of $PI(4,5)P_2$ might hinder further antibody adsorption. In
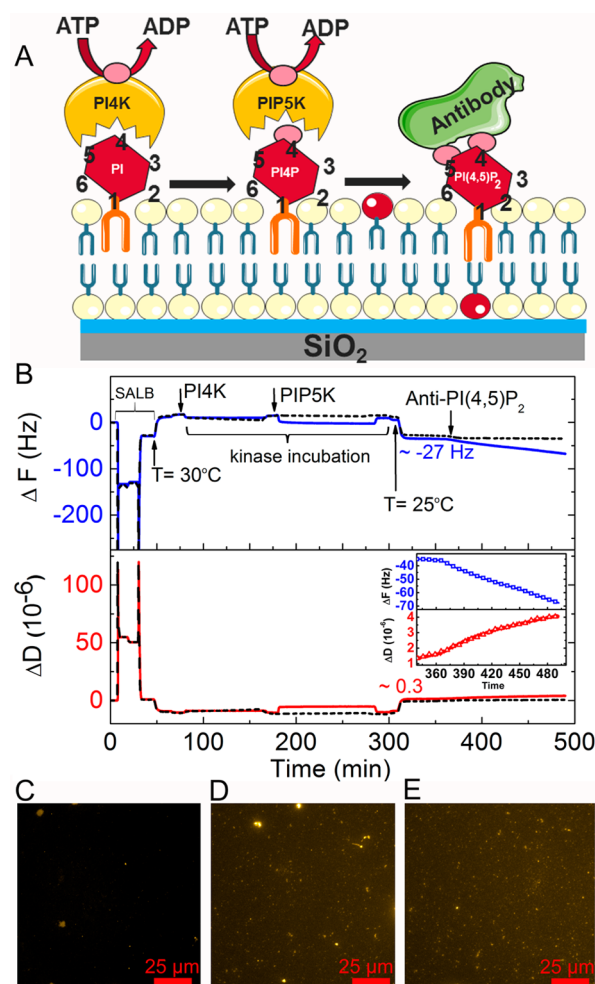
Figure 2. (A) Schematic illustration of steps involved in enzymatic conversion of PI to PI(4,5)P2. (B) QCM-D monitoring of $PI(4,5)P_2$ generation. The SALB procedure was performed at 25 °C to form DOPC bilayers with 10% PI followed by sequential incubation of the formed membrane with PI4KIIIβ and PIP5K1A at 30 °C. Anti-$PI(4,5)P_2$ antibody was then injected, leading to frequency change (blue trace). As a control, the same steps were repeated except the injection of PIP5K1A (dashed line). The inset in panel B represents the frequency and dissipation changes during antibody binding to bilayer treated with both enzymes. Background-corrected fluorescence micrographs of DOPC lipid bilayer doped with (C) 10% PI and (D) 10% $PI(4,5)P_2$, after incubation with fluorescently labeled anti-$PI(4,5)P_2$. (E) Background-corrected fluorescence micrograph of supported DOPC lipid bilayer (containing 10% PI) sequentially treated with PI4Kβ and PIP5Kα and incubated with fluorescently labeled anti-$PI(4,5)P_2$.

addition, the cluster formation might affect antigen accessibility which is known to affect the kinetics of antibody binding at the membrane interface.[25] Together, these effects would be predicted to result in an underestimate of the true amount of $PI(4,5)P_2$ produced, hence the actual conversion process may be even more efficient than estimated here and verifies that the SLB platform provides a suitable environment to support kinase activity.

Having established the above assays for in situ generation of phosphoinositides, we evaluated the effect of a pharmacologic inhibitor on such lipid kinase mediated generation of PI4P. A recently synthesized compound, STF-200211,[26] designed to inhibit PI4KIIIβ was tested at the indicated final concentrations

of inhibitor which are around its therapeutically relevant concentration range with an EC_{50} value of 174 nM. The same experimental procedure and condition as before was repeated, but in this case the enzyme was first preincubated with the inhibitor for 30 min at room temperature.

Following incubation of the kinase plus inhibitor, a solution of 5 μg/mL anti-PI4P antibody was added (see arrow in inset of Figure 3). The binding curves monitored by changes in ΔF
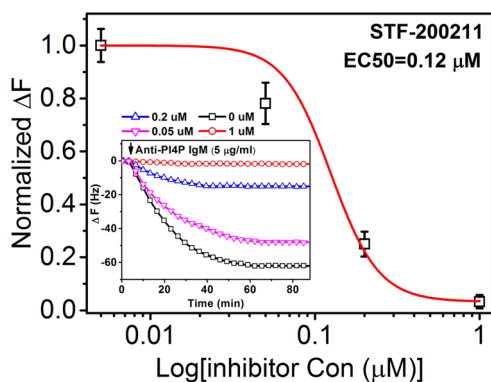
Figure 3. *In situ* antibody binding to PI4P generated by lipid kinase in the presence of a PI4K inhibitor. (A) Semi-log dose response curve and calculated EC_{50} value of a lipid kinase inhibitor. The inset shows the QCM-D frequency changes (ΔF) curves corresponding to binding of anti-PI4P to a PI-containing bilayer treated with PI4K in the presence of the indicated concentrations of inhibitor. The initial baseline values are the normalized frequency shifts for the bilayers (defined as ΔF Bilayer = 0). The observed negative frequency shift was due to antibody binding to the bilayer. The ΔF at each condition was normalized to the frequency change obtained in the absence of inhibitor. Calculated EC_{50} = 0.12 μM.

are shown in the inset of Figure 3. The kinetics of antibody binding shows significant reduction in the presence of increasing concentration of inhibitor and enabled a calculation of EC50 = 0.12 μM. This determination is comparable to that obtained in a standard solution based assay of PI4K activity (Figure S6). Interestingly, the latter format includes detergent in the assay buffer to optimize enzymatic activity.

In summary, using QCM-D, we demonstrate multienzyme catalytic phosphorylation of phosphatidylinositol (PI) in a SLB platform. We further utilize the PI4P containing SLB platform to demonstrate pharmacologic inhibition of PI4Kβ and calculation of a small molecule inhibitor's EC50 against PI4K. Our new lipid bilayer format assay appears to provide sufficiently more physiologic conditions such that exogenous addition of detergent is no longer required to optimize the lipid kinase activity while enabling label-free analysis of the membrane association step.

■ ASSOCIATED CONTENT

Ⓢ Supporting Information

The Supporting Information is available free of charge on the ACS Publications website at DOI: 10.1021/acs.analchem.6b01293.

Experimental details and additional supporting figures (Figures S1−S6) and supporting Table S1 (PDF)

■ AUTHOR INFORMATION

Corresponding Authors

*E-mail: jeffrey.glenn@stanford.edu.

*E-mail: njcho@ntu.edu.sg. Fax: (+65)67912274.

■ REFERENCES

(1) Balla, A.; Balla, T. *Trends Cell Biol.* **2006**, *16*, 351−361.

(2) de Graaf, P.; Zwart, W. T.; van Dijken, R. A.; Deneka, M.; Schulz, T. K.; Geijsen, N.; Coffer, P. J.; Gadella, B. M.; Verkleij, A. J.; van der Sluijs, P. *Mol. Biol. Cell* **2004**, *15*, 2038−2047.

(3) Knight, Z. A.; Feldman, M. E.; Balla, A.; Balla, T.; Shokat, K. M. *Nat. Protoc.* **2007**, *2*, 2459−2466.

(4) Demian, D. J.; Clugston, S. L.; Foster, M. M.; Rameh, L.; Sarkes, D.; Townson, S. A.; Yang, L.; Zhang, M.; Charlton, M. E. *J. Biomol. Screening* **2009**, *14*, 838.

(5) Nir, S.; Düzgüneş, N.; Bentz, J. *Biochim. Biophys. Acta, Biomembr.* **1983**, *735*, 160−172.

(6) Castellana, E. T.; Cremer, P. S. *Surf. Sci. Rep.* **2006**, *61*, 429−444.

(7) Baumann, M. K.; Amstad, E.; Mashaghi, A.; Textor, M.; Reimhult, E. *Biointerphases* **2010**, *5*, 114−119.

(8) Braunger, J. A.; Kramer, C.; Morick, D.; Steinem, C. *Langmuir* **2013**, *29*, 14204−14213.

(9) Dutta, D.; Pulsipher, A.; Luo, W.; Yousaf, M. N. *Analyst* **2014**, *139*, 5127−5133.

(10) Edvardsson, M.; Svedhem, S.; Wang, G.; Richter, R.; Rodahl, M.; Kasemo, B. *Anal. Chem.* **2009**, *81*, 349−361.

(11) Cho, N.-J.; Frank, C. W.; Kasemo, B.; Höök, F. *Nat. Protoc.* **2010**, *5*, 1096−1106.

(12) Jackman, J. A.; Cho, N.-J.; Duran, R. S.; Frank, C. W. *Langmuir* **2010**, *26*, 4103−4112.

(13) Janshoff, A.; Galla, H.-J.; Steinem, C. *Angew. Chem., Int. Ed.* **2000**, *39*, 4004−4032.

(14) Tabaei, S. R.; Choi, J.-H.; Haw Zan, G.; Zhdanov, V. P.; Cho, N.-J. *Langmuir* **2014**, *30*, 10363−10373.

(15) Tabaei, S. R.; Jackman, J. A.; Kim, S.-O.; Liedberg, B.; Knoll, W.; Parikh, A. N.; Cho, N.-J. *Langmuir* **2014**, *30*, 13345−13352.

(16) Keller, C.; Kasemo, B. *Biophys. J.* **1998**, *75*, 1397−1402.

(17) Catimel, B.; Ritter, G.; Welt, S.; Old, L. J.; Cohen, L.; Nerrie, M. A.; White, S. J.; Heath, J. K.; Demediuk, B.; Domagala, T.; Lee, F. T.; Scott, A. M.; Tui, G. F.; Jii, H.; Moritzi, R. L.; Simpsoni, R. J.; Burgess, A. W.; Nice, E. C. *J. Biol. Chem.* **1996**, *271*, 25664−25670.

(18) Rodahl, M.; Höök, F.; Fredriksson, C.; Keller, C. A.; Krozer, A.; Brzezinski, P.; Voinova, M.; Kasemo, B. *Faraday Discuss.* **1997**, *107*, 229−246.

(19) Jain, M. K.; Berg, O. G. *Biochim. Biophys. Acta, Lipids Lipid Metab.* **1989**, *1002*, 127−156.

(20) Barnett, S. F.; Ledder, L. M.; Stirdivant, S. M.; Ahern, J.; Conroy, R. R.; Heimbrook, D. C. *Biochemistry* **1995**, *34*, 14254−14262.

(21) Voinova, M. V.; Rodahl, M.; Jonson, M.; Kasemo, B. *Phys. Scr.* **1999**, *59*, 391.

(22) Patel, A. R.; Kanazawa, K. K.; Frank, C. W. *Anal. Chem.* **2009**, *81*, 6021−6029.

(23) Wang, Y.-H.; Collins, A.; Guo, L.; Smith-Dupont, K. B.; Gai, F.; Svitkina, T.; Janmey, P. A. *J. Am. Chem. Soc.* **2012**, *134*, 3387−3395.

(24) Czajkowsky, D. M.; Shao, Z. *Proc. Natl. Acad. Sci. U. S. A.* **2009**, *106*, 14960−14965.

(25) Jung, H.; Yang, T.; Lasagna, M. D.; Shi, J.; Reinhart, G. D.; Cremer, P. S. *Biophys. J.* **2008**, *94*, 3094−3103.

(26) Rutaganira, F. U.; Fowler, M. L.; McPhail, J. A.; Gelman, M. A.; Nguyen, K.; Xiong, A.; Dornan, G. L.; Tavshanjian, B.; Glenn, J. S.; Shokat, K. M.; Burke, J. E. *J. Med. Chem.* **2016**, *59*, 1830−1839.